

Effect of Multifactor on the Stability of Glucose Solution Emulsified Heavy Fuel Oil

Yu Wang, Zhenbin Chen,* Omar I. Awad, Wanjian Qin, and Umair Sultan

Cite This: *ACS Omega* 2023, 8, 34959–34971

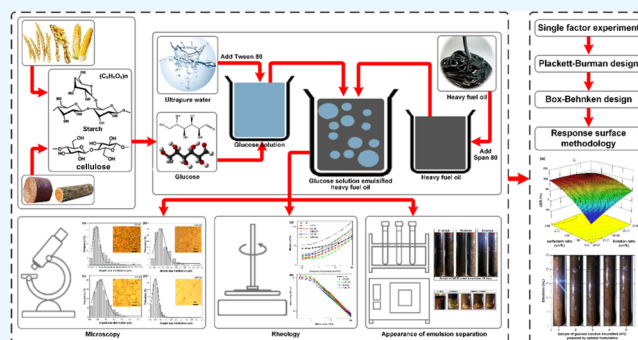
Read Online

ACCESS |

Metrics & More

Article Recommendations

ABSTRACT: Water emulsified heavy fuel oil (HFO) has been a promising alternative fuel for reducing oil consumption and preventing environmental pollution. However, the intrinsic challenges such as fuel formula, emulsion stability, and preparation process normally limit its further applications in energy-saving and emission reduction applications. In this study, the glucose obtained from biomass was added to a dispersed-phase aqueous solution of water emulsified HFO to prepare a novel alternative emulsified fuel. First, based on the preliminary experimental design, the effects of glucose and surfactant on the stability of the HFO emulsion were systematically evaluated through the appearance of emulsion separation, droplet size distribution, and rheological characteristics. It indicated that the surfactant ratio, hydrophilic–lipophilic balance value, solution ratio, and glucose/water ratio had significant impacts on emulsion stability. Subsequently, the optimum range of influencing factors of emulsion stability was determined by a single factor experiment and determined by the response surface methodology based on the Box–Behnken design; the optimal values of the above factors were 2.439 v/v%, 5.807, 26.462 v/v%, and 35.729%, respectively. Under these conditions, an optimal glucose solution emulsified HFO with a uniform brown color and long-term stability was obtained, making the unseparated emulsion ratio reach 98% (lasting for 7 days at 85 °C). Meanwhile, it emerged that the influence of multifactor on emulsion stability was not a simple linear correlation, and there were significant interactions between the solution ratio and the surfactant ratio, as well as between the glucose/water ratio and the surfactant ratio.



1. INTRODUCTION

Heavy fuel oil (HFO) is widely used in many fields including thermal power plants, metallurgical industry, and ocean transportation due to its attractive combination of attributes such as high heating value and low cost.^{1,2} Therefore, such a combination of attributes has high potential for being utilized in diesel-powered shipping in international trade. Nevertheless, the practical application of HFO still poses inevitable problems such as negative cold flow characteristics, poor fuel atomization, and incomplete combustion, which are caused by the high viscosity (700 mm²/s at 50 °C) and consequent difficulty in flowability.^{3–5} Moreover, various pollutants are emitted, such as carbon dioxide (CO₂), carbon monoxide (CO), nitrogen oxides (NO_x), and particulate matter (PM), when burning HFO, which limits its further applications.^{6,7} Therefore, it is of great significance to improve the fuel components to facilitate further engineering applications, including increasing engine performance and reducing emissions.

As an alternative fuel, water emulsified fuel has attracted considerable attention due to its remarkable advantages including suppressing NO_x and soot pollutants, improving the economic advantages,^{8,9} as well as no modification required when used in marine engines.^{10–12} Maiboom et al.¹³

demonstrated that the atomization and combustion performance of water emulsified fuel had improved compared with HFO, which could be attributed to microexplosion and secondary atomization. In addition, it is also promising for blending clean renewable fuels, such as bioethanol and glycerol, to reduce traditional fuel consumption and pollutant emissions.^{14–18} Nour et al.¹⁸ reported a reduction in NO_x and opacity emissions and an increase in CO and HC emissions for all higher alcohol/diesel blends tested, based on adding higher alcohols (butanol, octanol, and heptanol) to diesel. Zhang et al.¹⁶ prepared glycerol emulsified diesel fuel successfully, and it was found that the temperature and surfactant had a more significant influence on emulsion stability compared with the stirring speed and time. Therefore, in order to alleviate the shortage of fossil fuels and improve the low heating value of

Received: June 21, 2023

Accepted: August 23, 2023

Published: September 12, 2023



water emulsified fuel, it is of great research value to add biomass fuels to the dispersed-phase water of the HFO emulsion.

As a type of renewable biomass fuel, glucose is a corrosion-inhibiting and water-soluble polyol.¹⁹ In particular, it can be converted to gaseous H₂, CO, CH₄, and CO₂ in supercritical water, which may benefit the combustion process.^{20,21} In our previous work, glucose solution emulsified diesel was prepared by adding glucose into water emulsified diesel, which exhibited a remarkable emulsion stability (342 h at room temperature). The engine results indicated that it could improve the brake thermal efficiency at 2000 rpm and decrease NO_x emissions when burning glucose solution emulsified diesel,²² which proved the feasibility of using glucose solution emulsified fuel in diesel engines. In order to promote the large-scale application, the stability of glucose solution emulsified fuel needs to be further improved. In the subsequent work, we performed a single factor experiment considering the solution ratio, glucose/water ratio, surfactant ratio, and hydrophilic–lipophilic balance (HLB) value to evaluate the emulsification characteristics and stability of glucose solution emulsified HFO.²³ The results showed that both the emulsion stability and homogeneity had a trend of increasing first and then decreasing as the glucose/water ratio changed from 0 to 40%. The droplet size of water-in-oil (W/O) emulsions decreased by adding the glucose since the introduction of polyols could reduce the interfacial tension and equalize the refractive indices of the phase interface.^{24,25} Differently, the added glucose to the aqueous phase of HFO emulsions increased the density difference between the dispersed and continuous phases, which could accelerate the separation of the emulsion and, in turn, decrease the emulsion stability. Thus, it is urgent to prepare a glucose solution emulsified HFO with excellent stability by optimizing the emulsification process based on the above results, which can facilitate its application in marine diesel engines.

There are many input process parameters that can affect the stability of glucose solution emulsified HFO to varying degrees, including HLB, emulsifier concentration, water concentration, additive concentration, emulsification duration, emulsification temperature, stirring speed with time duration, and cosolvent concentration.^{20,22,23,26} Nevertheless, it is highly challenging to fit all process parameters into one equation due to process complexity, wherein a series of formulations, processes, and storage parameters are involved, which make it difficult to predict the emulsification process. Therefore, different techniques should be applied including unit nonlinear regression, factor analysis, and response surface methodology (RSM) to model and optimize the emulsification parameters so as to meet the requirement of preparing a superior emulsion.^{27,28} Among them, the Plackett–Burman design of screen factors and the RSM are quite effective for three-dimensional model construction, which are mature and reliable methods for optimizing emulsion preparation parameters.^{29,30} RSM is a collection of mathematical and statistical techniques based on polynomial equations, which perform statistical predictions on a data set by fitting experimental data. It is used to design experiments, establish models, evaluate the impact of variables, and search for the optimal conditions for variables to predict target reactions. RSM is an important branch of experimental design and a key tool for developing new processes, optimizing performance, and improving new product designs and formulations.³¹

In this work, the stable glucose solution emulsified HFO was prepared successfully by process optimization based on the preliminary experiments, single factor experiments, Plackett–

Burman design experiments, and RSM based on Box–Behnken design experiments. The interfacial viscoelasticity, shear viscosity, and stability of HFO emulsions were investigated in detail from the perspective of rheology, and the droplet size distribution statistics and the emulsion stability were analyzed simultaneously. A relationship between the preparation process parameters and the stability of glucose solution emulsified HFO was established.

2. EXPERIMENTAL SECTION

2.1. Emulsion Preparation. During the emulsion preparation, the RMG 180 HFO purchased from the fuel oil station was used, and ultrapure water (18.25 MΩ cm resistivity) was prepared by the HK-UP-II-40 analytical laboratory ultrapure water machine (Haokang Technology, China). Span 80 (chemically pure), Tween 80 (chemically pure), and glucose (analytically pure) were purchased from Guangzhou Chemical Reagent Factory. The detailed properties of RMG 180, glucose, and Span 80 are shown in Tables 1–3, respectively.

Table 1. Detailed Properties of RMG 180³²

param.	test method	RMG 180
density (20 °C)	ISO 12185:1996	940 kg/m ³
cetane number	ASTM D613	40.96
API		14.38°
elemental analysis	ASTM D5291-16	
H		11.97 wt %
C		88.03 wt %
H/C		1.62 wt %
composition	SH/T0659-1998	
paraffin		10.6 wt %
naphthene		28.5 wt %
1-ring aromatics		20.3 wt %
2-ring aromatics		13.7 wt %
≥ 3-ring aromatics		16.5 wt %
unidentified aromatics		2.8 wt %
asphaltene		7.6 wt %

The preparation procedure and observation testing method of the emulsion are described in Figure 1. First, glucose was added into the ultrapure water and stirred for 5 min with a speed of 200 rpm and a room temperature of 20–28 °C so as to dissolve the glucose completely. Then, Tween 80 was added to the glucose solution and Span 80 was added to HFO and stirred for 3 min, separately. Next, Tween 80-dissolved glucose solution and Span 80-dissolved HFO were stirred for 5 min for mixing. Subsequently, the mixture was heated for 5 min in an oil bath and stirred in the oil bath until a homogeneous emulsion formed. Lastly, the emulsion was transferred into a 25 mL glass test tube for further observation and analysis. In this study, the HLB value of the emulsion is calculated as

$$HLB_{\text{emulsion}} = \varphi_S \times HLB_S + \varphi_T \times HLB_T \quad (1)$$

where HLB_S and HLB_T indicate the HLB values of Span 80 and Tween 80, respectively. φ_S and φ_T indicate the mass fractions of mixed surfactant of Span 80 and Tween 80, respectively.

2.2. Emulsion Stability. Emulsion stability is usually defined as the period between emulsion formation and separation.^{20,23} Since there is inevitable error when observing the separation time, the unseparated emulsion ratio (UER, %) was introduced to evaluate the emulsion stability by utilizing the

Table 2. Detailed Properties of Glucose³³

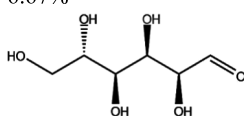
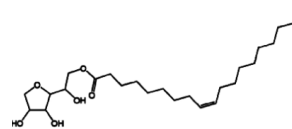
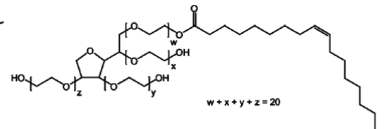
Glucose	
Param.	
Chemical formula	C ₆ H ₁₂ O ₆
Density	1.5620 g cm ⁻³ (at 18°C)
Melting point	150°C
Flash point	202.243°C
heating value	15.6 MJ/kg
oxygen content	53.33%
carbon content	40%
hydrogen content	6.67%
Structural formula	
Solubility	
Solubility in water	Very soluble
Temperature (°C)	Solubility in grams of glucose per 100 mL of water
25	91
30	125
50	244
70	357
90	556

Table 3. Detailed Properties of Span 80 and Tween 80^{34,35}

Param.	Span 80	Tween 80
Chemical formula	C ₂₄ H ₄₄ O ₆	C ₃₂ H ₆₀ O ₁₀
Density	1.06 g/mL	0.99 g/mL
Ionic property	Non-ionic	Non-ionic
HLB value	4.3	15
Structural formula		

relative volume method. In this study, the UER is calculated in eq 2

$$\text{UER} = \frac{\text{volume occupied by the unseparated emulsion layer}}{\text{total volume of the whole emulsion in a test tube}} \times 100 \quad (2)$$

2.3. Experimental Baseline. The default value of influencing factors in all experiments was set as follows: 30% v/v solution ratio (30% v/v—100 mL of glucose solution emulsified HFO emulsion contains 30 mL of a glucose aqueous solution), 40% v/v glucose/water ratio (40%—40 g of glucose is added into 100 g of ultrapure water), 2 v/v% surfactant ratio, the HLB value was 6.3, the emulsification duration was 10 min, the emulsification temperature was 80 °C, and the stirring speed was 500 rpm. All of the test tube samples were kept motionless and in an XMTA-600 thermostatic oven (01–1B) at 85 °C for 7 days (except for the preliminary experiment), and the separation phenomenon of each group was recorded. The emulsion

stability was represented as UER in all experiments, which were run in triplicate, and the average values were adopted.

2.4. Preliminary Experiment. The preliminary experiment was a test based on microscopy, rheological techniques, and the appearance of emulsion separation. The emulsion samples were prepared and stored at room temperature for 2 days for microscopic examination and a rheological test.

In the emulsion droplet size test, to further visualize the emulsion microstructure maintaining the shape and droplet size, the cover glass was not used. The image of the sample (50× objective) was observed by a Leica DMRX polarized optical microscope (Leica, Germany). The droplet size distribution (DSD) was analyzed on ImageJ 1.8.0 software by intercepting the microscopic image of 700 × 700 pixels, including the following image processing steps: binarizing to highlight the low luminance interfaces, filling holes in water droplets, segmenting continuous droplets, and removing all incomplete droplets that touch the image boundary. Subsequently, the area of each

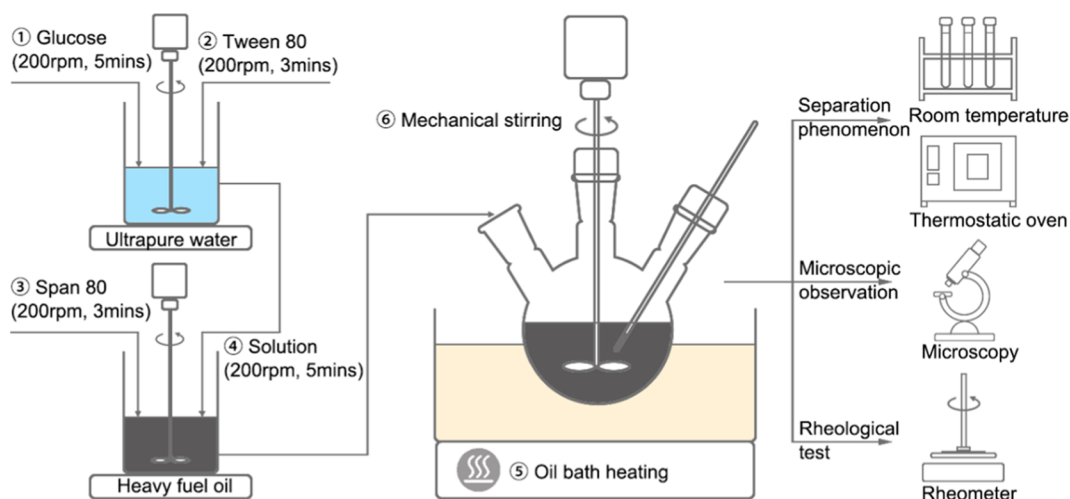


Figure 1. Preparation procedure and observation testing method of the emulsion.

droplet was cumulatively summed to calculate the mean droplet size (MDS) and DSD.

In terms of rheological testing, the interfacial rheological behavior of the emulsion was studied by using Discovery HR-30 (Waters LLC, America) at 25 °C. The gap between the parallel plate and the sample stage (diameter, $d = 60$ mm) was set to 0.45 mm. The samples needed to be changed for each test. Flow continuous shear measurements were carried out at the shear frequency of 0.01–100 s^{-1} to record the interfacial viscosity. Oscillatory shear rheological measurements were carried out at a fixed frequency of 10 rad/s (from 0.01 to 100 strain %) to determine the upper limit of the linear viscoelastic region, and then, the frequency scanning measurement was conducted under a strain amplitude of 0.1% in the linear and coelastic range.

In order to observe the appearance of emulsion separation, all test tube samples were kept in an XMTA-600 thermostatic oven (01–1B) at 85 °C for 28 days and at room temperature (20–28 °C) for 60 days; the separation phenomenon of each group was observed and recorded.

2.5. Single Factor Experiment. The single factor experiment means that only a single factor changes to different levels for comparison, while other factors are strictly consistent in the whole test. The single factor experiment provides a reasonable data range to determine the optimal level of each factor for the Plackett–Burman design. The multifactor involved in the experiment included the solution ratio, glucose/water ratio, surfactant ratio, HLB value, emulsification duration, emulsification temperature, and stirring speed.

2.6. Plackett–Burman Experimental Design. The Plackett–Burman design is an effective technique for optimizing media components, and it is often used to evaluate the effects of multifactor.^{30,36} The Plackett–Burman design was carried out with the statistical software Design Expert 10.0.4, and the results were fitted by a first-order model as follows:

$$Y = \beta_0 + \sum_i \beta_i X_i (i, j = 1, 2, 3, \dots, k) \quad (3)$$

In the formula, Y is the estimated objective function (herein, it is the unseparated emulsion ratio, UER), X_i is the coded independent factor, β_0 is the model intercept, and β_i is the regression coefficient.

2.7. Box–Behnken Design and Response Surface Methodology. The Box–Behnken design was utilized to

further investigate the optimal level points for key factors in predicting response.³⁰ The experimental design was concluded by the statistical software Design Expert 10.0.4, and the obtained results were analyzed using the ANOVA of the RSM. The RSM based on the Box–Behnken design was fitted by the following equation

$$Y = \beta_0 + \sum_i \beta_i X_i + \sum_{ii} \beta_{ii} X_i^2 + \sum_{ij} \beta_{ij} X_i X_j (i, j = 1, 2, 3, \dots, k) \quad (4)$$

In the formula, Y is the predictive response (herein, it is the unseparated emulsion ratio, UER), $X_i X_j$ are the coding independent variables, β_0 is the offset term, β_i is the linear relationship coefficient, β_{ii} is the quadratic relationship coefficient, and β_{ij} is the interactive relationship coefficient.

3. RESULTS AND DISCUSSION

3.1. Preliminary Experiment. To explore the effect of adding glucose and surfactants on the emulsion system, a preliminary experiment was performed based on microscopy, rheological techniques, and the appearance of emulsion separation. The composition ratio of the emulsion prepared by the preliminary experiment is shown in Table 4. In water

Table 4. Preliminary Experiment Scheme

factors	solution ratio	glucose/water ratio	surfactant ratio	HLB value	HFO ratio
units	v/v%	%	v/v%		v/v%
G0-S0	30	0	0		70
G40-S0	30	40	0		70
G0-S2	30	0	2	6.3	68
G40-S2	30	40	2	6.3	68

emulsified HFO emulsions, G0-S0 refers to no added glucose and surfactant; G40-S0 refers to added glucose but no added surfactant; G0-S2 refers to no added glucose but added surfactant; and G40-S2 refers to added glucose and surfactant. The appearance of each sample was observed to evaluate the emulsion stability at room temperature and in an 85 °C thermostat oven. It was found that the emulsion with glucose and surfactant exhibited no emulsion separation after 60 days at room temperature, as shown in Figure 2, which indicated that

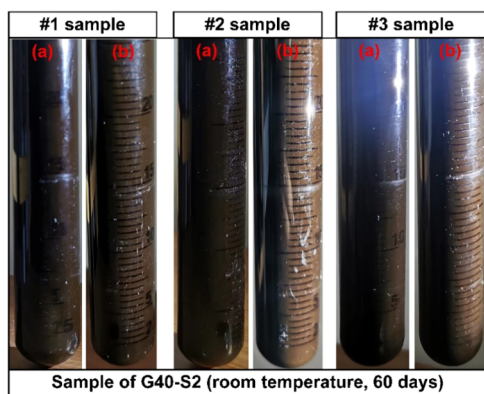


Figure 2. Appearance of three samples of the G40-S2 emulsion at room temperature: (a) initial appearance of the sample preparation, (b) appearance after 60 days of sample preparation.

the emulsion had excellent transportability and storage properties. However, the emulsion separation phenomenon occurred within 7 days in an 85 °C thermostat oven, as shown in Figure 3. The appearance, including oil-layer separation, water-layer separation, and separation transition, suggested that it was difficult to assess the emulsion stability only by the relative volume ratio of the separated oil layer or the separated water layer, and the UER was more suitable for emulsion stability.

3.1.1. Droplet Size Distribution and Mean Droplet Size. The photomicrographs and histograms of the DSD of the emulsion are depicted in Figure 4. From Figure 4a,b, it was found that the DSD corresponding to the curve peaks of G0-S0 and G40-S0 was similar, but the curve peaks of G40-S0 were higher, and the histogram distribution range and MDS were smaller. This indicated that the DSD uniformity was slightly improved after adding glucose to the emulsion without a surfactant. From Figure 4c,d, it can be seen that the DSD corresponding to the curve peak of G40-S2 was smaller, the curve peak was higher, the histogram distribution range was narrower, and the MDS was smaller. This indicated that the added glucose to the emulsion with surfactant also could improve the DSD uniformity. As reported in previous studies, the added glucose increases the strength of the emulsion interfacial film³⁷ and slightly reduces the droplet size of the emulsion,²⁴ thus leading to an improved emulsion stability. Similarly, comparing Figures 4a,c and 4b,d, respectively, it could be found that compared with the emulsion without a surfactant, the DSD of the emulsion with a surfactant was more uniform and the MDS was smaller. The reason for this phenomenon is that the added surfactants can reduce the interfacial tension, which makes the MDS of the dispersed phase smaller and the DSD more homogeneous, thus leading to an increase in emulsion stability.^{24,38,39} In addition, compared with the slight improvement effect after adding glucose on the DSD

uniformity and MDS of the emulsion, the degree of improvement of surfactant addition is more significant.

3.1.2. Interfacial Shear Viscosity and Modulus. The results of rheological tests of glucose solution emulsified HFO are shown in Figure 5. Figure 5a characterizes the effect of glucose and surfactant on the interface viscoelasticity of the emulsion (G' is the storage modulus, G'' is the loss modulus). The storage modulus and loss modulus represent the elasticity and viscosity of the emulsion system to a certain extent, respectively. In the angular frequency range (0.1–100 Hz), the G'' of each group was significantly larger than G' , indicating that the interface manifested in each component emulsion had a viscous characteristic. It can be concluded that there is no large-scale adsorption of glucose at the interface, and thus, no specific structure with high mechanical strength that affects the viscous characteristic of the emulsion is formed.

In Figure 5b, the interfacial shear viscosity of each group presented a downward trend with the increase in shear rate due to the spatial repulsion between droplets to stabilize the droplets as the droplets were randomly distributed in the initial stage of equilibrium. As the shear rate increased, the droplets became organized on the flow line, thereby reducing the interfacial shear viscosity.⁴⁰ The curves of G40-S0 vs G0-S0 and G40-S2 vs G0-S2 showed minimal differences in interfacial shear viscosity, implying that glucose had almost no effect on the interfacial shear viscosity of the emulsion. Since the interfacial shear viscosity of the curve G0-S2 was always lower than that of G0-S0, and that of G40-S2 was also lower than that of G40-S0, it meant that the interfacial shear viscosity slightly decreased with the added surfactants. This phenomenon could be attributed to the fact that the added surfactant reduced the interfacial tension and further reduced the interfacial shear viscosity.³⁸ Notably, the interfacial shear viscosity of each component emulsion at a shear rate of 1 s⁻¹ was as follows: G40-S0 > G0-S0 > HFO > G40-S2 > G0-S2, reflecting that the effect of increasing glucose on interfacial shear viscosity was less obvious than the decreasing surfactant.

3.1.3. Appearance of Emulsion Separation. In order to accelerate emulsion separation and compare the UER better for emulsion stability evaluation, each component sample was observed and recorded in an 85 °C thermostatic oven (28 days). Figure 6 depicts the appearance of emulsion separation with different components in an 85 °C thermostatic oven (28 days). It could be found that G0-S0 had barely obvious separation within 28 days; however, G40-S0 had complete separation within 7 days. This phenomenon could be ascribed to the larger density difference between the internal and external phases caused by the high glucose content of 40%, which accelerated the emulsion separation process. The UER of G40-S2 was higher than that of G0-S2 within 28 days, which could be attributed to

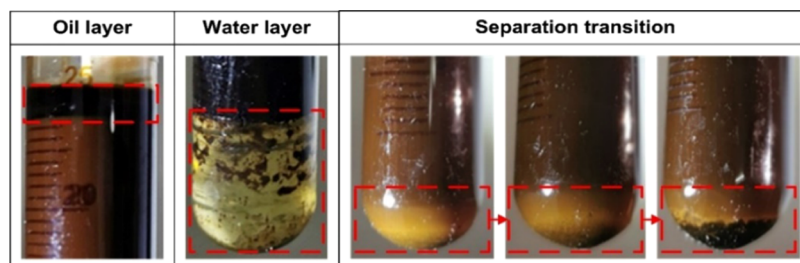


Figure 3. Appearance of emulsion separation at 85 °C (7 days): oil-layer separation, water-layer separation, and separation transition.

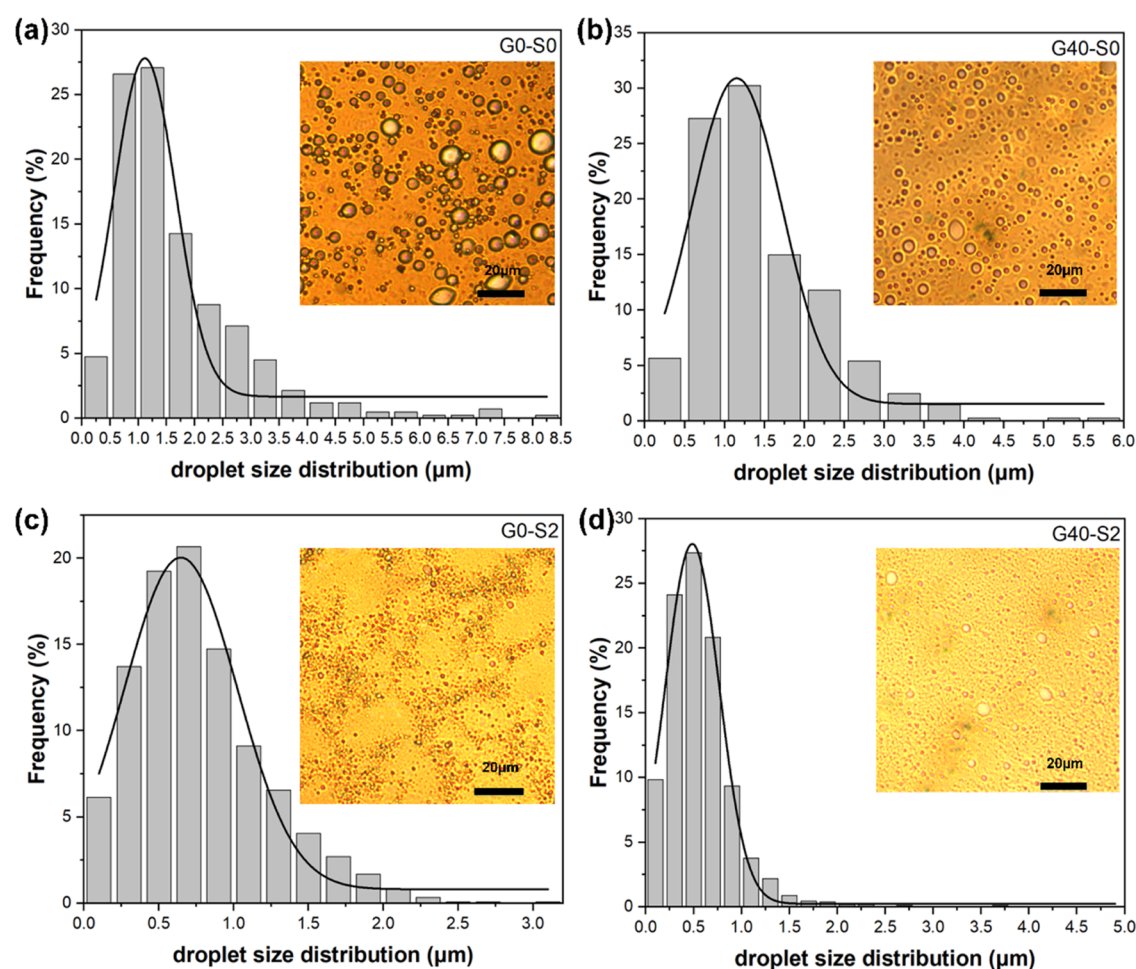


Figure 4. Photomicrographs and histograms of DSD of different components: (a) G0-S0, (b) G40-S0, (c) G0-S2, and (d) G40-S2.

the glucose substitution for partial water, further reducing the interfacial tension between the aqueous and oil phases, thereby improving the formation process.²⁵ In addition, G40-S0 vs G0-S0 and G40-S2 vs G0-S2 displayed that the added surfactant made the emulsion appearance brown. G0-S2 emulsion separation occurred within 7 days when compared with G0-S0; the result suggests that the combination of added surfactants and many natural surfactants in HFO can increase the surfactant content in an emulsion, leading to the condensation and sedimentation of surfactants at the bottom of the container.²³

G40-S2 vs G40-S0 showed that adding surfactants to the emulsion containing glucose could decrease the emulsion separation rate, which may be due to the added surfactant molecules tending to concentrate on the W/O interface, where the interfacial activity increases and enhances the interfacial film, reducing the interfacial tension between the W/O two phases, increasing the W/O interfacial viscosity, decreasing the droplet aggregation rate, and improving the emulsion stability.^{24,39}

Combined with the above results regarding the microscopic features, rheological features, and appearance of emulsion separation, the surfactant was needed to prepare glucose solution emulsified HFO with better emulsion stability. Previous studies have demonstrated that water, surfactant, HLB value, and additive had considerable effects on emulsion stability.^{20,38,41–43} However, it is necessary to further investigate the parameters obtained from the preliminary experiment, which significantly affected the emulsion separation significantly.

Besides, the effect of emulsification temperature, emulsification duration, and stirring speed on emulsion stability should also be analyzed in depth.

3.2. Single Factor Experiment and Plackett–Burman Design. **3.2.1. Determine the Level Scope for Multifactor by Single Factor Experiment.** The single factor experiment was carried out to determine the effects of multifactor on emulsion stability. The emulsion preparation scheme for the single factor experiment is expressed in Table S, and the results are shown in Figure 7. It was noted that in the solution ratio of 10–30 v/v%, the UER increased synchronously. However, at 30–40 v/v%, the increase of UER was not significant. Therefore, it could be concluded that the critical value for the solution ratio level was 30 v/v%. Similarly, the surfactant ratio, HLB value, glucose/water ratio, emulsification temperature, and emulsification duration were determined to be 2 v/v%, 6.3, 30%, 60 °C, and 30 min, respectively. Especially when the glucose/water ratio is 10%, the UER is higher than 20%. That may be because when only a small amount of glucose is added, its glucose is completely dissolved in the water phase so that the refractive index of the internal phase (water phase) is increased to be close to the refractive index of the external phase (oil phase), realizing the balance of the refractive index of the two immiscible phases, reducing the attraction between emulsion droplets, thus preventing flocculation and coalescence, thereby improving the stability of the emulsion and increasing the UER. However, when the glucose/water ratio increases to 30%, the UER is

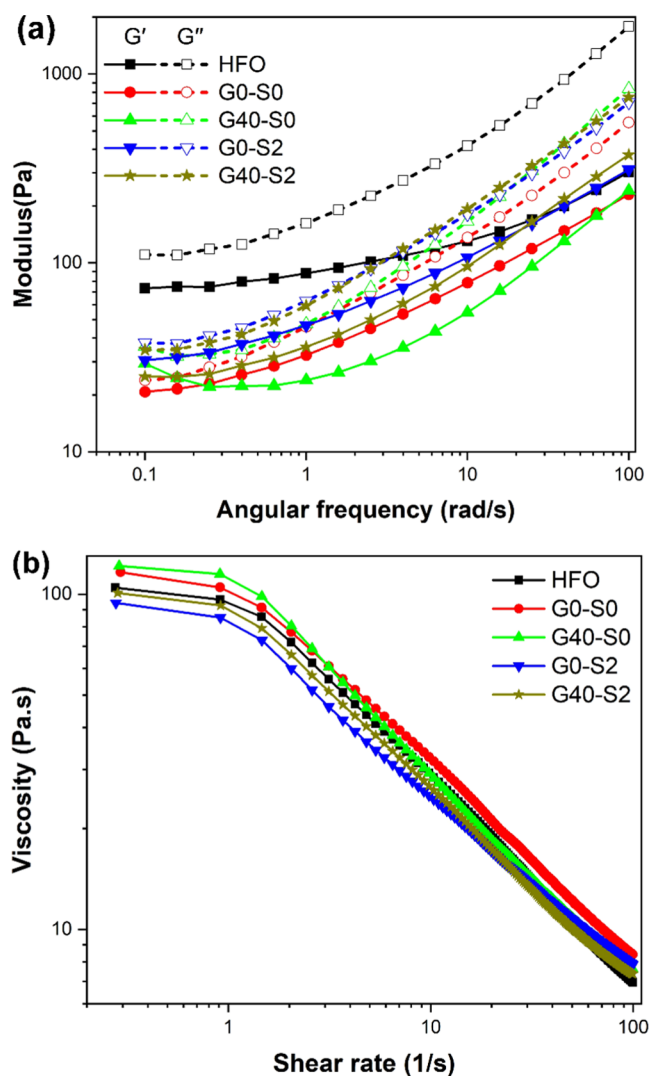


Figure 5. (a) Interfacial storage modulus G' (filled symbols) and loss modulus G'' (empty symbols) between oil and water as functions of angular frequency at different samples. (b) Interfacial viscosity as a function of shear frequency between oil and water at different samples.

higher than 20%. That may be because when a certain amount of glucose is added, some of its glucose is dissolved in the water phase, and some of it is adsorbed on the newly formed W/O interface film in coordination with the surfactant, which reduces the W/O interface tension, thus improving the emulsion stability and increasing the UER.²⁵ Furthermore, when the stirring speed was changed from 200 to 500 rpm, the curve tended to be flat, but the curve gradually increased as the stirring speed was increased from 500 to 1100 rpm, indicating that the critical value for the stirring speed was 500 rpm. These findings suggest that the optimal level scopes of the solution ratio, glucose/water ratio, surfactant ratio, HLB value, emulsification duration, emulsification temperature, and stirring speed were determined as 20–40 v/v %, 20–40%, 1–3 v/v%, 4.3–8.3, 40–80 °C, 10–50 min, and 200–800 rpm, respectively.

3.2.2. Selection of Significant Variables by the Plackett–Burman Experiment Design. The multivariate screening was performed first to determine the factor that had a significant influence on UER among the multifactor. The upper and lower limits of each factor variable were selected based on the single factor level experiment, as revealed in Table 6. In the Plackett–

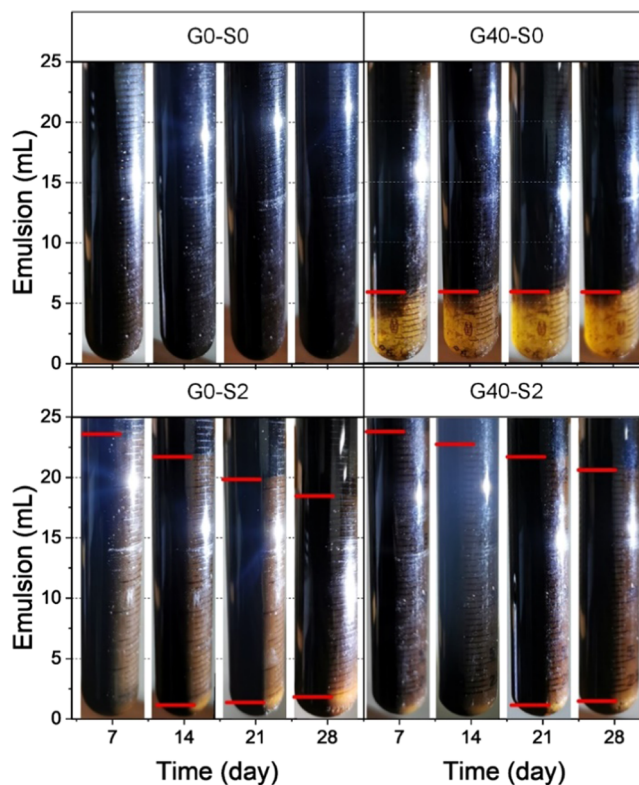


Figure 6. Appearance of emulsion separation of different components in an 85 °C (28 days) thermostat oven: G0-S0, G40-S0, G0-S2, and G40-S2.

Burman design of 12 trials, each variable had two levels and the corresponding Y (UER), as shown in Table 9.

To approach the neighborhood of the optimal response, the first-order fitting model of UER was obtained from the Plackett–Burman design, expressed as follows

$$Y = +54.75 + 8.75X_1 - 8.58X_2 + 29.92X_3 - 14.75X_4 + 0.92X_5 - 2.58X_6 - 0.083X_7 \quad (5)$$

where Y is the estimated objective function UER and X_1 , X_2 , X_3 , X_4 , X_5 , X_6 , and X_7 are the coded values of the solution ratio, glucose/water ratio, surfactant ratio, HLB value, emulsification duration, emulsification temperature, and stirring speed, respectively. The coefficient of each variable in eq 4 represents the effecting degree of the variable on the UER. The linear regression coefficient R^2 of the model was 0.9713, and the adjusted determination coefficient ($Adj R^2$) was 0.9211, indicating that the model was reasonable for the Plackett–Burman design. The influence of each variable and the statistical analysis of the results are listed in Table 6. According to the P -value and F -value in Table 6, the influence of multifactor on the UER was as follows: surfactant ratio > HLB value > solution ratio > glucose/water ratio > emulsification duration > stirring speed > emulsification temperature. In general, factors with a P -value less than 0.05 are considered to have a significant effect on emulsion stability. Therefore, the significant variables including the solution ratio, glucose/water ratio, surfactant ratio, and HLB value were selected for further optimization research, and the remaining insignificant variables were ignored.

3.3. Box–Behnken Design and Response Surface Methodology. To further examine the optimal level point of the key factors (solution ratio, glucose/water ratio, surfactant

Table 5. Single Factor Experiment Scheme

group	solution ratio	glucose/water ratio	surfactant ratio	HLB value	emulsification temperature	emulsification duration	stirring speed
units	v/v%	%	v/v%		°C	min	rpm
1	10	40	2	6.3	80	10	500
2	20	40	2	6.3	80	10	500
3	30	40	2	6.3	80	10	500
4	40	40	2	6.3	80	10	500
5	30	10	2	6.3	80	10	500
6	30	20	2	6.3	80	10	500
7	30	30	2	6.3	80	10	500
8	30	40	1	6.3	80	10	500
9	30	40	3	6.3	80	10	500
10	30	40	4	6.3	80	10	500
11	30	40	5	6.3	80	10	500
12	30	40	2	4.3	80	10	500
13	30	40	2	8.3	80	10	500
14	30	40	2	10.3	80	10	500
15	30	40	2	12.3	80	10	500
16	30	40	2	14.3	80	10	500
17	30	40	2	6.3	20	10	500
18	30	40	2	6.3	40	10	500
19	30	40	2	6.3	60	10	500
20	30	40	2	6.3	80	30	500
21	30	40	2	6.3	80	50	500
22	30	40	2	6.3	80	70	500
23	30	40	2	6.3	80	10	200
24	30	40	2	6.3	80	10	800
25	30	40	2	6.3	80	10	1100

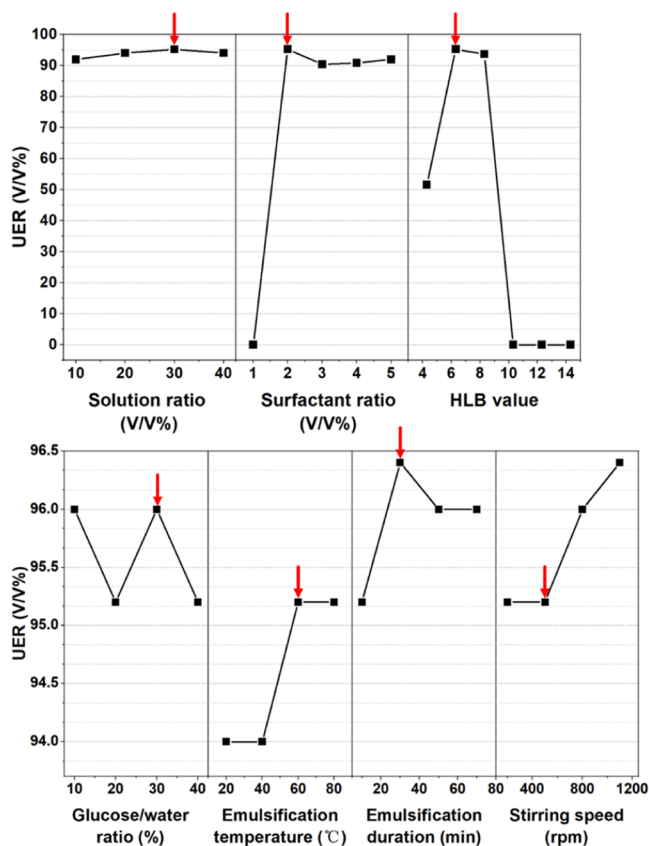


Figure 7. Effect of solution ratio, glucose/water ratio, surfactant ratio, HLB value, emulsification duration, emulsification temperature, and stirring speed on the UER.

ratio, and HLB value) on the UER, the Box–Behnken design and RSM were applied to optimize these crucial input parameters in the emulsification process. The low-level and high-level codes for each factor in the Box–Behnken design were designed based on the above results, as shown in Table 7. The Box–Behnken design of 29 trials with three levels of each variable and the corresponding Y (UER) are given in Table 10. The experimental data were fitted by the regression analysis, resulting in the following second-order polynomial equation model

$$\begin{aligned}
 Y = & 96.00 + 13.83X_1 - 7.67X_2 + 30.67X_3 + 14.17X_4 \\
 & + 0.00X_1X_2 - 24.00X_1X_3 - 4.50X_1X_4 + 23.00X_2X_3 \\
 & - 3.00X_2X_4 + 4.00X_3X_4 - 6.83X_1^2 + 2.42X_2^2 \\
 & - 20.58X_3^2 - 29.83X_4^2
 \end{aligned} \quad (6)$$

where Y is the predictive response UER and X_1 , X_2 , X_3 , and X_4 are the coded values of solution ratio, glucose/water ratio, surfactant ratio, and HLB, respectively.

The variance analysis (ANOVA) reveals the significance of each experimental variable and its interactions; meanwhile, it determines the influence degree of each variable on the response.⁴⁴ Table 8 shows the ANOVA results for the quadratic regression analysis model for the UER of glucose solution emulsified HFO. In statistics, when the P -value is less than 0.05, whereas the F -value is large, the model is considered highly significant.⁴⁵ It could be found that the P -value of the experimental model was below 0.01, and the F -value reached 4.99, suggesting that the experimental model was extremely significant. Besides, the unfit item was not significant (0.1590 for P -value). In general, the model fits well when the determination coefficient is higher than 0.75, which indicates that the model

Table 6. Plackett–Burman Design Screening Variables and Statistical Analysis of the Influence of Each Variable on the UER^a

factor	name of parameters	units	low level	high level	coefficient	standard error	F-value	P-value
X ₁	solution ratio	v/v%	20	40	8.75	3.06	8.1606	0.0461*
X ₂	glucose/water ratio	%	20	40	−8.58	3.06	7.8527	0.0487*
X ₃	surfactant ratio	v/v%	1	3	29.92	3.06	95.3967	0.0006*
X ₄	HLB value		4.3	8.3	−14.75	3.06	23.1895	0.0086*
X ₅	emulsification temperature	°C	40	80	0.92	3.06	0.0896	0.7796
X ₆	emulsification duration	min	10	50	−2.58	3.06	0.7113	0.4465
X ₇	stirring speed	rpm	200	800	−0.08	3.06	0.0007	0.9796

^aR² = 0.9713, R² (Adj) = 0.9211. *Significant at 95% confidence degree ($P < 0.05$).

Table 7. Low and High Coding Values for Each Key Factor in the Box–Behnken Design

factors	name of parameters	units	type	minimum	maximum	coded values	mean
X ₁	solution ratio	v/v%	numeric	20	40	−1 = 20, 1 = 40	30
X ₂	glucose/water ratio	%	numeric	20	40	−1 = 20, 1 = 40	30
X ₃	surfactant ratio	v/v%	numeric	1	3	−1 = 1, 1 = 3	2
X ₄	HLB value		numeric	4.3	8.3	−1 = 4.3, 1 = 8.3	6.3

Table 8. ANOVA for the UER According to the Response Surface Quadratic Model^a

variable	statistical analysis				
	sum of squares	df	mean square	F-value	P-value
model	29323.21	14	2094.51	4.99	0.0024*
X ₁	2296.33	1	2296.33	5.48	0.0346*
X ₂	705.33	1	705.33	1.68	0.2156
X ₃	11285.33	1	11285.33	26.91	0.0001*
X ₄	2408.33	1	2408.33	5.74	0.0311*
X ₁ X ₂	3.638 × 10 ^{−012}	1	3.638 × 10 ^{−012}	8.675 × 10 ^{−015}	1.0000
X ₁ X ₃	2304.00	1	2304.00	5.49	0.0344*
X ₁ X ₄	81.00	1	81.00	0.19	0.6670
X ₂ X ₃	2116.00	1	2116.00	5.05	0.0413*
X ₂ X ₄	36.00	1	36.00	0.086	0.7738
X ₃ X ₄	64.00	1	64.00	0.15	0.7019
X ₁ ²	302.88	1	302.88	0.72	0.4097
X ₂ ²	37.88	1	37.88	0.090	0.7682
X ₃ ²	2748.15	1	2748.15	6.55	0.0227*
X ₄ ²	5773.15	1	5773.15	13.77	0.0023*
cor total	35194.21	28			

^aR² = 0.8332, R² (Adj) = 0.6664. *Significant at 95% confidence degree ($P < 0.05$).

can explain the corresponding response variation.⁴⁶ Therefore, the 0.8332 for the determination coefficient R^2 , obtained from the regression equation of the ANOVA, suggested that the model could explain 83.32% of the response change. The 0.6664 for the correction coefficient R^2 (Adj) indicated that the model applicability was not perfect enough; however, it did not affect the factor analysis on UER using the model. The ultrahigh emulsion stability of glucose solution emulsified HFO could lead to less difference in response values, slightly higher errors, and a slightly lower coefficient, which were attributed to the high content of resin and asphaltene in HFO, making the variation value of response values (UER) less obvious. In general, resin and asphaltene are easily combined into micelles,⁴¹ and they form aggregates with rigid structures wrapped by water droplets through interacting with other particles at the water droplet interface.⁴⁷ This could cause an increase in emulsion stability and a decrease in the magnitude of the factor change value.

Notably, the P -values can reflect the interaction strength between variables in addition to testing the significance of the variables.⁴⁸ The smaller the P -value, the more significant the corresponding variable is. Table 8 shows that all of the

parameters, including the primary terms X₂ (glucose/water ratio), X₄ (HLB value), interactive terms X₁X₃ (solution ratio and surfactant ratio), X₂X₃ (glucose/water ratio and surfactant ratio), and quadratic terms X₃² (the quadratic term of the surfactant ratio), had significant effects ($P < 0.05$), while the effects of X₃ (surfactant ratio) and X₄² (the quadratic term of the HLB value) were extremely significant ($P < 0.01$). These indicated that the influence of various factors on UER was not a simple linear relationship. The relationship of four factors affecting UER in the experiment was as follows (consistent with the significant factors of the Plackett–Burman design): surfactant ratio > HLB value > solution ratio > glucose/water ratio. The relationship of the interaction intensity was as follows: X₁X₃ > X₂X₃ > X₁X₄ > X₃X₄ > X₂X₄ > X₁X₂. In particular, the P -value of X₃ was much less than 0.01–0.0001, indicating that the surfactant ratio played a decisive role in emulsion stability in multifactor influence. The P -values for X₁X₃ (0.0344) and X₂X₃ (0.0413) were less than 0.05, indicating that the interaction strengths between the solution ratio and the surfactant ratio, as well as between the glucose/water ratio and the surfactant ratio, were quite high. That is, their effects on UER were more

dependent, which could be ascribed to the presence of a large number of asphaltenes and resins that acted as natural surfactants in the HFO, making the emulsions contain a high concentration of surfactants overall.²³ The surfactant molecules were adsorbed on the oil–water interface to form a viscoelastic interfacial film to resist the agglomeration of emulsion droplets, resulting in the stability of the emulsion system being decisively influenced by the surfactant.²⁴

To further analyze the optimal level value of each variable and the interaction between the variables, a three-dimensional response surface plot was constructed by plotting the response (UER) to any two independent variables on the Z-axis. Meanwhile, the other variables were kept at optimal levels. The 3D response surface curve with significant interaction is shown in Figure 8. The response surface diagram drawn by the regression equation directly reflected the influence degree of each factor on the response value.⁴⁹ Figure 8 depicts the 3D

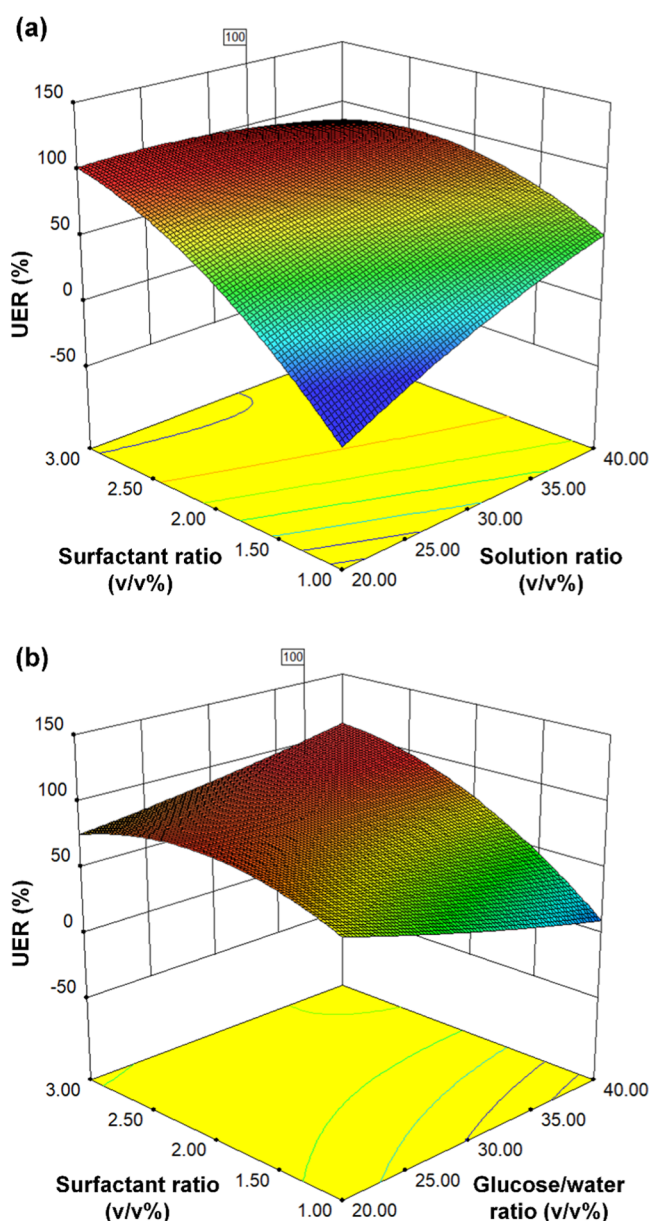


Figure 8. Response surface plot showing the effects of (a) surfactant ratio and solution ratio and (b) surfactant ratio and glucose/water ratio.

response surface curves of the solution ratio to the surfactant ratio and the glucose/water ratio to the surfactant ratio with significant interactions, respectively. The results showed that the response surface of Figure 8 was convex, which indicated that the optimal conditions were well-defined and there was a maximum value for UER. However, compared with Figure 8b, Figure 8a displays a more elliptical shape, suggesting that the interaction between the solution ratio and the surfactant ratio was more significant, which was consistent with the Box–Behnken design. (The *P*-value of 0.0344 for X_1X_3 was less than that of 0.0413 for X_2X_3 .) According to the response surface analysis, the emulsion optimal formula was obtained by numerical optimization of experimental results: 2.439 v/v% for surfactant ratio, 5.807 for HLB value, 26.462 v/v% for solution ratio, and 35.729% for glucose/water ratio; the predicted maximum UER reached up to 99% when other variables retained the default value.

The integer value of the optimal formula obtained by software optimization (surfactant ratio 2.4 v/v%, HLB value 5.8, solution ratio 26.5 v/v%, and glucose/water ratio 35.7%) was taken for experimental validation, and the obtained UER reached 98% based on the five parallel tests. The appearance of five samples of glucose solution emulsified HFO prepared by the optimal formulation is shown in Figure 9; uniform brown could be

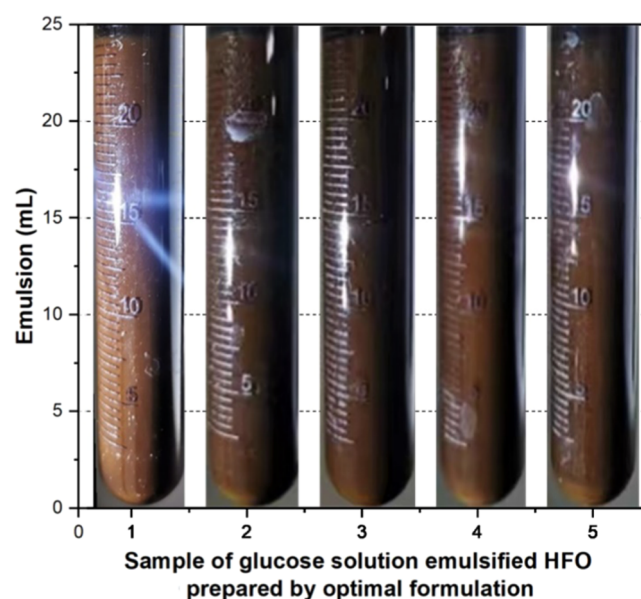


Figure 9. Appearance of five samples of glucose solution emulsified HFO prepared by the optimal formulation.

observed in the prepared emulsion with the optimal formula. Compared with the theoretical prediction, there was a certain relative error in the repeatable experiment. After keeping the test sample in the thermostat oven for 7 days, there was no separated water layer at the bottom of the glass test tube, but about 0.3–0.5 mL of separated oil layer appeared at the top, slightly darkened. These results suggested that the emulsion prepared by the optimal formula changed inapparently, further verifying the correctness of the optimal formula from an experimental perspective.

4. CONCLUSIONS

This research aimed to examine the process of preparing a glucose solution emulsified heavy fuel oil (HFO) by using

Table 9. Level Code for Each Variable in the Plackett–Burman Design and the Estimated Objective Function of UER

factor:	1	2	3	4	5	6	7	
	coded variable level							
run	X_1	X_2	X_3	X_4	X_5	X_6	X_7	UER Y (%)
1	-1	1	1	1	-1	-1	-1	56
2	-1	-1	1	-1	1	1	-1	92
3	1	-1	-1	-1	1	-1	1	62
4	-1	1	-1	1	1	-1	1	0
5	1	-1	1	1	-1	1	1	90
6	-1	-1	-1	-1	-1	-1	-1	42
7	1	1	-1	1	1	1	-1	0
8	-1	1	1	-1	1	1	1	86
9	1	-1	1	1	1	-1	-1	94
10	1	1	1	-1	-1	-1	1	90
11	-1	-1	-1	1	-1	1	1	0
12	1	1	-1	-1	-1	1	-1	45

Table 10. Level Code for Each Variable in the Box–Behnken Design and the Corresponding Response of UER

factor	1	2	3	4	
	coded variable level				response UER
run	X_1	X_2	X_3	X_4	Y (%)
1	-1	0	0	1	60
2	-1	-1	0	0	96
3	0	0	0	0	96
4	1	-1	0	0	96
5	0	0	-1	1	0
6	0	0	0	0	96
7	0	0	0	0	96
8	0	-1	0	1	96
9	0	0	0	0	96
10	1	0	0	-1	54
11	1	0	-1	0	96
12	0	0	1	-1	90
13	0	1	1	0	94
14	0	0	1	1	96
15	0	-1	1	0	96
16	0	-1	-1	0	94
17	0	1	0	1	94
18	0	0	-1	-1	10
19	-1	0	-1	0	0
20	1	0	1	0	96
21	-1	0	1	0	96
22	-1	1	0	0	94
23	1	0	0	1	86
24	0	-1	0	-1	44
25	0	0	0	0	96
26	-1	0	0	-1	10
27	0	1	0	-1	54
28	0	1	-1	0	0
29	1	1	0	0	94

various formulations and preparation conditions. The characterization and detailed analysis of emulsion stability were conducted, taking into account the influence of glucose, surfactants, and other relevant parameters. The primary findings derived from our study may be succinctly expressed as follows.

- The addition of surfactants and glucose resulted in enhanced emulsion stability under ambient conditions, hence prolonging the duration of stability to over 60 days. Nevertheless, the phenomenon of emulsion separation was seen to take place within a period of 7 days when subjected to a thermostat oven operating at a temperature of 85 °C. This observation underscores the crucial role of temperature in influencing the stability of emulsions. Surfactants exerted a significant influence on the improvement of both droplet size distribution (DSD) uniformity and mean droplet size (MDS) of the emulsion. In the angular frequency range (0.1–100 Hz), the G'' of each group was considerably larger than G' , indicating that the interface manifested in each component emulsion had a viscous characteristic. The interfacial shear viscosity decreased slightly with the added surfactants, but it decreased significantly with the increase of the shear rate. However, the added glucose had almost no effect on the interfacial shear viscosity. Overall, the impact of glucose on interfacial shear viscosity was smaller compared to surfactants.
- The effect of multiple variables on emulsion stability was assessed using single factor experiments, the Plackett–Burman design, and response surface methodology (RSM) using the Box–Behnken design. The primary contributing factors discovered in this study were surfactant ratio, HLB value, solution ratio, and glucose/water ratio. The impact of these factors on the uniformity of emulsion ratio (UER) was found to be nonlinear, and notable interactions were identified between the solution ratio and the surfactant ratio, as well as the glucose/water ratio and the surfactant ratio. The ideal formula for emulsion preparation was discovered, leading to the attainment of a uniform brown appearance and high stability. This resulted in a uniformity of emulsion response (UER) of 98%, which was observed to persist for a duration of 7 days at a temperature of 85 °C.

This work represents the first comprehensive optimization of the process parameters involved in the synthesis of emulsified HFO by using a glucose solution. Additional research is necessary to explore the spray characteristics, combustion performance, and economic assessment of the ideal glucose solution emulsified HFO. Although a few interesting results have been obtained thus far, these aspects will be the focus of future investigations.

■ AUTHOR INFORMATION

Corresponding Author

Zhenbin Chen – School of Mechanics and Electronics Engineering, Hainan University, Haikou 570228, P. R. China; orcid.org/0000-0003-4348-3754; Phone: +86 898 6626 7922; Email: zhenbin1208@hainanu.edu.cn; Fax: +86 898 6626 7576

Authors

Yu Wang – School of Mechanics and Electronics Engineering, Hainan University, Haikou 570228, P. R. China; National Engineering Research Center for Small and Special Precision Motors, Guiyang 550081, P. R. China

Omair I. Awad – School of Mechanics and Electronics Engineering, Hainan University, Haikou 570228, P. R. China; orcid.org/0000-0001-7453-6690

Wanjian Qin – National Engineering Research Center for Small and Special Precision Motors, Guiyang 550081, P. R. China
Umair Sultan – Faculty of Agricultural Biosystems Engineering and Technology, MNS University of Agriculture, Multan 60000, Pakistan

Complete contact information is available at:

<https://pubs.acs.org/10.1021/acsomega.3c04416>

Notes

The authors declare no competing financial interest.

ACKNOWLEDGMENTS

The work in this paper was supported by the National Natural Science Foundation of China (Grant No. 51866002).

REFERENCES

- (1) Iliuta, I.; Iliuta, M. C. Modeling of SO₂ seawater scrubbing in countercurrent packed-bed columns with high performance packings. *Sep. Purif. Technol.* **2019**, *226*, 162–180.
- (2) Nielsen, R. F.; Haglind, F.; Larsen, U. Design and modeling of an advanced marine machinery system including waste heat recovery and removal of sulphur oxides. *Energy Convers. Manage.* **2014**, *85*, 687–693.
- (3) Ampah, J. D.; Liu, X.; Sun, X.; Pan, X.; Xu, L.; Jin, C.; et al. Study on characteristics of marine heavy fuel oil and low carbon alcohol blended fuels at different temperatures. *Fuel* **2022**, *310*, No. 122307.
- (4) McGill, R.; Remley, W.; Winther, K. Alternative fuels for marine applications A Report from the IEA Advanced Motor Fuels Implementing Agreement 2013, p 54.
- (5) Atabani, A.; Silitonga, A.; Ong, H.; Mahlia, T.; Masjuki, H.; Badruddin, I. A.; Fayaz, H. Non-edible vegetable oils: a critical evaluation of oil extraction, fatty acid compositions, biodiesel production, characteristics, engine performance and emissions production. *Renewable Sustainable Energy Rev.* **2013**, *18*, 211–245.
- (6) Park, H. Y.; Han, K.; Kim, H. H.; Park, S.; Jang, J.; Yu, G. S.; Ko, J. H. Comparisons of combustion characteristics between bioliquid and heavy fuel oil combustion in a 0.7 MWth pilot furnace and a 75 MWE utility boiler. *Energy* **2020**, *192*, 116557.
- (7) Henaug, C.; Stenersen, D.; Norrdal, T. Possible hazards for engines and fuel systems using heavy fuel oil in cold climate Report prepared for Norwegian Maritime Authority/PAME Ramboll/Marintek 2016.
- (8) Mondal, P. K.; Mandal, B. K. A comprehensive review on the feasibility of using water emulsified diesel as a CI engine fuel. *Fuel* **2019**, *237*, 937–960.
- (9) Khatri, D.; Goyal, R. Performance, emission and combustion characteristics of water diesel emulsified fuel for diesel engine: A review. *Mater. Today: Proc.* **2020**, *28*, 2275–2278.
- (10) Christopher, Y.; Van Tongeren, M.; Urbanus, J.; Cherrie, J. W. An assessment of dermal exposure to heavy fuel oil (HFO) in occupational settings. *Ann. Occup. Hyg.* **2011**, *55* (3), 319–328, DOI: 10.1093/annhyg/mer002.
- (11) Feng, L.; Du, B.; Tian, J.; Long, W.; Tang, B. J. E. Combustion Performance and Emission Characteristics of a Diesel Engine Using a Water-Emulsified Heavy Fuel Oil and Light Diesel Blend. *Energies* **2015**, *8* (12), 13628–13640.
- (12) Zadyanova, N. M.; Skvortsova, Z. N.; Traskin, V. Y.; Yampol'skaya, G. P.; Mironova, M. V.; Frenkin, E. I.; et al. Heavy oil as an emulsion: Composition, structure, and rheological properties. *Colloid J.* **2016**, *78* (6), 735–746.
- (13) Maiboom, A.; Tauzia, X. NO_x and PM emissions reduction on an automotive HSDI Diesel engine with water-in-diesel emulsion and EGR: An experimental study. *Fuel* **2011**, *90* (11), 3179–3192.
- (14) Manzetti, S.; Andersen, O. A review of emission products from bioethanol and its blends with gasoline. Background for new guidelines for emission control. *Fuel* **2015**, *140*, 293–301.
- (15) Lin, C.-Y.; Tsai, S.-M. Emulsification characteristics of nano-emulsions of solketal in diesel prepared using microwave irradiation. *Fuel* **2018**, *221*, 165–170.
- (16) Zhang, M.; Wu, H. Stability of emulsion fuels prepared from fast pyrolysis bio-oil and glycerol. *Fuel* **2017**, *206*, 230–238.
- (17) Eaton, S. J.; Harakas, G. N.; Kimball, R. W.; Smith, J. A.; Pilot, K. A.; Kuflik, M. T.; Bullard, J. M. Formulation and Combustion of Glycerol–Diesel Fuel Emulsions. *Energy Fuels* **2014**, *28* (6), 3940–3947.
- (18) Nour, M.; Attia, A. M. A.; Nada, S. A. Combustion, performance and emission analysis of diesel engine fuelled by higher alcohols (butanol, octanol and heptanol)/diesel blends. *Energy Convers. Manage.* **2019**, *185*, 313–329.
- (19) Kılınççeker, G.; Doğan, T. The influences of glucose on corrosion behaviour of copper in chloride solution. *Prot. Met. Phys. Chem. Surf.* **2016**, *52* (5), 910–920.
- (20) Sun, J.; Chen, Z.; Liu, J.; Liu, S.; Wang, X. Optimization on preparation process parameters of glucose solutions emulsified diesel. *Trans. Chin. Soc. Agric. Eng.* **2015**, *31* (1), 228–235.
- (21) DEMİRBAŞ, A. Bioethanol from Cellulosic Materials: A Renewable Motor Fuel from Biomass. *Energy Sources* **2005**, *27* (4), 327–337.
- (22) Chen, Z.; Li, K.; Liu, J.; Wang, X.; Jiang, S.; Zhang, C. Optimal design of glucose solution emulsified diesel and its effects on the performance and emissions of a diesel engine. *Fuel* **2015**, *157*, 9–15.
- (23) Chen, Z.; Wang, L.; Wei, Z.; Wang, Y.; Deng, J. Effect of components on the emulsification characteristic of glucose solution emulsified heavy fuel oil. *Energy* **2022**, *244*, 123147.
- (24) Zhu, Q.; Pan, Y.; Jia, X.; Li, J.; Zhang, M.; Yin, L. Review on the Stability Mechanism and Application of Water-in-Oil Emulsions Encapsulating Various Additives. *Compr. Rev. Food Sci. Food Saf.* **2019**, *18* (6), 1660–1675, DOI: 10.1111/1541-4337.12482.
- (25) Benichou, A.; Aserin, A.; Garti, N. Polyols, High Pressure, and Refractive Indices Equalization for Improved Stability of W/O Emulsions for Food Applications. *J. Dispersion Sci. Technol.* **2001**, *22* (2–3), 269–280.
- (26) Sartomo, A.; Santoso, B.; Muraza, O. Recent progress on mixing technology for water-emulsion fuel: A review. *Energy Convers. Manage.* **2020**, *213*, No. 112817, DOI: 10.1016/j.enconman.2020.112817.
- (27) Bendjaballah, M.; Canselier, J. P.; Oumeddour, R. Optimization of oil-in-water emulsion stability: experimental design, multiple light scattering, and acoustic attenuation spectroscopy. *J. Dispersion Sci. Technol.* **2010**, *31* (9), 1260–1272, DOI: 10.1080/01932690903224888.
- (28) Traynor, M.; Burke, R.; Frias, J. M.; Gaston, E.; Barry-Ryan, C. Formation and stability of an oil in water emulsion containing lecithin, xanthan gum and sunflower oil. *Int. Food Res. J.* **2013**, *20* (5), 2173–2181, DOI: 10.21427/d7d189.
- (29) Boateng, I. D.; Yang, X.-M. Process optimization of intermediate-wave infrared drying: Screening by Plackett–Burman; comparison of Box–Behnken and central composite design and evaluation: A case study. *Ind. Crops Prod.* **2021**, *162*, No. 113287, DOI: 10.1016/j.indcrop.2021.113287.
- (30) Zhang, N.; Bénard, P.; Chahine, R.; Yang, T.; Xiao, J. Optimization of pressure swing adsorption for hydrogen purification based on Box–Behnken design method. *Int. J. Hydrogen Energy* **2021**, *46* (7), 5403–5417.
- (31) Körbahti, B. K.; Rauf, M. A. Response surface methodology (RSM) analysis of photoinduced decoloration of toluidine blue. *Chem. Eng. J.* **2008**, *136* (1), 25–30.
- (32) Wu, Z.; Mao, Y.; Yu, L.; Wang, S.; Xia, J.; Qian, Y.; Lu, X. Surrogate Formulation for Marine Diesel Considering Some Important Fuel Physical–Chemical Properties. *Energy Fuels* **2019**, *33* (4), 3539–3550.
- (33) Shendurse, A. M.; Khedkar, C. D. Glucose: Properties and Analysis. *Encyclopedia Food Health* **2016**, 239–247.
- (34) Koneva, A. S.; Safonova, E. A.; Kondrakhina, P. S.; Vovk, M. A.; Lezov, A. A.; Chernyshev, Y. S.; Smirnova, N. A. Effect of water content on structural and phase behavior of water-in-oil (n-decane) micro-

emulsion system stabilized by mixed nonionic surfactants SPAN 80/TWEEN 80. *Colloids Surf., A* **2017**, *518*, 273–282.

(35) Xu, Y.; Hellier, P.; Purton, S.; Baganz, F.; Ladommatos, N. Algal biomass and diesel emulsions: An alternative approach for utilizing the energy content of microalgal biomass in diesel engines. *Appl. Energy* **2016**, *172*, 80–95.

(36) Gao, J.; Xu, H.; Li, Q.-j.; Feng, X.-h.; Li, S. Optimization of medium for one-step fermentation of inulin extract from Jerusalem artichoke tubers using *Paenibacillus polymyxa* ZJ-9 to produce R,R-2,3-butanediol. *Bioresour. Technol.* **2010**, *101* (18), 7076–7082.

(37) Feng, X.; Behles, J. A. Understanding the Demulsification of Water-in-Diluted Bitumen Froth Emulsions. *Energy Fuels* **2015**, *29* (7), 4616–4623.

(38) Preetika, R.; Mehta, P. S.; Kaisare, N. S.; Basavaraj, M. G. Kinetic stability of surfactant stabilized water-in-diesel emulsion fuels. *Fuel* **2019**, *236*, 1415–1422.

(39) Kokal, S. Crude-Oil Emulsions: A State-Of-The-Art Review. *SPE Prod. Facil.* **2005**, *20*, 5–13, DOI: 10.2118/77497-PA.

(40) Maurya, N. K.; Mandal, A. Investigation of synergistic effect of nanoparticle and surfactant in macro emulsion based EOR application in oil reservoirs. *Chem. Eng. Res. Des.* **2018**, *132*, 370–384.

(41) da Silva, M.; Sad, C. M. S.; Pereira, L. B.; Corona, R. R. B.; Bassane, J. F. P.; dos Santos, F. D.; et al. Study of the stability and homogeneity of water in oil emulsions of heavy oil. *Fuel* **2018**, *226*, 278–285.

(42) Liu, D.; Li, C.; Yang, F.; Sun, G.; You, J.; Cui, K. Synergetic effect of resins and asphaltenes on water/oil interfacial properties and emulsion stability. *Fuel* **2019**, *252*, 581–588.

(43) Farooq, A.; Shafaghat, H.; Jae, J.; Jung, S. C.; Park, Y. K. Enhanced stability of bio-oil and diesel fuel emulsion using Span 80 and Tween 60 emulsifiers. *J. Environ. Manage.* **2019**, *231*, 694–700.

(44) Roshan, N.; Ghader, S.; Rahimpour, M. R. Application of the response surface methodology for modeling demulsification of crude oil emulsion using a demulsifier. *J. Dispersion Sci. Technol.* **2018**, *39* (5), 700–710.

(45) Abdulredha, M. M.; Hussain, S. A.; Abdullah, L. C. Optimization of the demulsification of water in oil emulsion via non-ionic surfactant by the response surface methods. *J. Pet. Sci. Eng.* **2020**, *184*, No. 106463, DOI: 10.1016/j.petrol.2019.106463.

(46) Reddy, L. V. A.; Wee, Y.-J.; Yun, J.-S.; Ryu, H.-W. Optimization of alkaline protease production by batch culture of *Bacillus* sp. RKY3 through Plackett–Burman and response surface methodological approaches. *Bioresour. Technol.* **2008**, *99* (7), 2242–2249.

(47) Sullivan, A. P.; Kilpatrick, P. K. The effects of inorganic solid particles on water and crude oil emulsion stability. *Ind. Eng. Chem. Res.* **2002**, *41* (14), 3389–3404, DOI: 10.1021/ie010927n.

(48) Liu, J.-Z.; Weng, L.-P.; Zhang, Q.-L.; Xu, H.; Ji, L.-N. Optimization of glucose oxidase production by *Aspergillus niger* in a benchtop bioreactor using response surface methodology. *World J. Microbiol. Biotechnol.* **2003**, *19*, 317–332.

(49) Xinran, Z.; Weiguang, L.; Xujin, G.; Wenbiao, F.; Pengfei, R. Optimization on combined UV/chlorine process for removal of ammonia in drinking water. *CIESC J.* **2014**, *65* (3), 1049–1055.